Geosystems and Geoenvironment 2 (2023) 100130

Contents lists available at ScienceDirect

Geosystems and Geoenvironment

journal homepage: www.elsevier.com/locate/geogeo

Earthquake hotspot and coldspot: Where, why and how?

Subodh Chandra Pal[a,*], Asish Saha[a], Indrajit Chowdhuri[a], Dipankar Ruidas[a], Rabin Chakrabortty[a], Paramita Roy[a], Manisa Shit[b]

[a] Department of Geography, The University of Burdwan, Bardhaman, West Bengal 713104, India

[b] Department of Geography, Raiganj University, Uttar Dinajpur, Raiganj, West Bengal 733134, India

ARTICLE INFO

Article history:
Received 11 April 2022
Revised 21 July 2022
Accepted 30 August 2022

Handling Editor: A. Vasanthi

Keywords:
Tectonic activities
Earthquake
Hotspot
Coldspot
GIS

ABSTRACT

Global tectonic activities are playing an important role in the occurrences of devastating earthquakes and related long-term changes in the earth's system surface. However, the plate tectonics processes and their interaction with the earth's crust are very much complex, and it is a subject of unending debate. Therefore, tectonism-induced landslide, tsunami, liquefaction, and fire are significant earthquake-related hazards, which have a larger potential and overwhelming impact on life and infrastructural properties throughout the world. In this study, we have emphasized the identification of earthquake hotspot and coldspot zones considering historical earthquake data across the plate boundary of the world. Here, a total of 7773 historical earthquake points were collected as input parameters with three-moment magnitude (M_w) classes (<4.5, 4.5–6.0, and >6.0). Two statistical methods namely hotspot analysis (Getis-Ord GI*) and optimized hotspot analysis were used in the detection of global earthquake hotspot and coldspot zones using the geographic information system (GIS) platform. Hotspot and coldspot zone are identified under 99%, 95%, and 90% confidence levels. Alongside, here we have also discussed the paradigm, evidence of tectonic, and historical earthquakes, and how and why they are formed with the help of the existing theoretical constraints. The result indicates that the Pacific ring of fire, Peru-Chile Trench, and the mid-Atlantic oceanic ridge is fall in the hotspot zones of 99%, 95%, and 90% confidence levels.

1. Introduction

Earth has been subjected to several devastating natural hazards over the course of geological time, the most destructive and frightening of which are earthquakes. This natural phenomenon is a major manifestation of the power of tectonic forces caused by the thermal condition of the earth's interior. It manifests itself by shaking the earth's surface with seismic waves caused by a sudden release of strain in the earth's crust's outer layer that has grown over a long duration. According to Strahler and Strahler (1976), "the oscillation and vibration generated by disturbance of gravitational equilibrium of rocks beneath the earth's surface cause deadly earthquakes". Earthquakes are caused by the vibration of the earth caused by rupture and the abrupt displacement of rocks beyond their elasticity limits (Hamblin, 1975). The forces produced by plate movements have shaped the earth for hundreds of millions of years, resulting in several earthquake hotspots and cold spots around the world, it usually happens as a result of fault slippage produced by friction between various tectonic plates; however, volcanic eruptions and human explosions can also be a source of earthquakes. Several studies on asthenosphere plate movements (Gulia and Wiemer, 2010; Kusky, 2008; Lomnitz, 2013; Nur and Cline, 2000), volcanic activity (Eggert and Walter, 2009; Jones and Malone, 2005), and anthropogenic activities (Albano et al., 2017; Mulargia and Bizzarri, 2014; Wilson et al., 2017) suggest how they are associated with earthquake from ancient time to recent era. Several elements, including hotspot and coldspot zones on the earth's surface, are thought to play distinct roles in influencing the size, types, and location of earthquakes. When tectonic plates slide beneath one another due to gravity force, a great quantity of energy is released, culminating in the most destructive earthquakes (Rychert and Harmon, 2021). According to Pritchard et al. (2013), a massive earthquake can cause thermal anomalies, ground deformation, hydrological changes, and additional earthquakes or eruptions in volcanic regions hundreds of kilometers away from the epicenter; the Andes southern volcanic zone experienced such an eruption in the same years as the Chile earthquake in 1906 and 1960 (Watt et al., 2009). The massive mega thrust earthquake in Sumatra (26 December, 2004) with a Mw of 9.3 generated the most devastating tsunami caused by the subduction of the Indian plate beneath the Burma plate, making it the

* Corresponding author.
E-mail address: geo.subodh@gmail.com (S.C. Pal).

https://doi.org/10.1016/j.geogeo.2022.100130
2772-8838/

second largest life-threatening catastrophic event in world history after the Chile earthquake in 1960 (Ghobarah et al., 2006). Aceh's coastline in Indonesia was devastated by tsunami waves of up to 35 m in height just 15 min after the quake (Frankenberg et al., 2020; Monecke et al., 2008). The seismic magnitude is proportional to the average amount of slip, the product of the rupture area, and the efficient shear modules (Aki, 1966), and Bassett et al. (2016) explain how the structure and frictional properties of the over thrusting plates control seismogenic behavior. The subduction of the Pacific plate under northeast Japan at a rate of 8–9 cm/yr makes numerous large thrust earthquakes near the site of the Kurile-Japan Trench (DeMets et al., 1990). Transient slip events near the Japan-Kurile Trench caused the Tokachi Oki earthquakes in 1952, 1968, and 2003, as well as the Nemuro Oki earthquake in 1973 (Miyazaki et al., 2004). A supershear rupture of the Palu-Koro fault caused an earthquake with a Mw of 7.5 in central Sulawesi, Indonesia on September 28, 2018 (Bao et al., 2019). This strike slip fault has a high slip rate of ~42 mm/yr (Socquet et al., 2006), resulting in initial damage with rapid wave inundation in Palu, where a landslide later became accountable for 4350 estimated casualties (Bradley et al., 2019). San Andreas Fault between the North American plate and North Pacific Plate (earthquake in 1857, M_W ~7.9; 1906, Mw ~7.9) and North Anatolian Fault between the Eurasian plate and Anatolian plate (earthquake in 1992, M_W ~6.8) are notable examples of right lateral Strike slip fault resulting in small to high magnitude earthquake (Ghanbari and Saberi, 2006). According to Avouac et al. (2015)'s Nepal earthquake (M_W ~7.8) study, large earthquakes can be produced by releasing strain caused by the unzipping of pre seismically locked faults. The Chi-Chi earthquake in central Taiwan on September 21, 1999, with a Mw of 7.3 caused by the reactivation of the Chelungpu Fault, resulted in a major landslide (Lin et al., 2004). Frictional qualities of plates are heavily influenced by the type and characteristics of the surface; for example, the position of highly conductive Seamounts in the New Zealand subduction zone resulted in volcanic eruptions and earthquakes (Rychert and Harmon, 2021). Critically stressed faults cause earthquakes during permanent and dynamic stress changes (Hill et al., 1993); for example, the Denali, Alaska earthquake increased seismicity throughout British Columbia in 2002. Ridgecrest earthquake in 2019 is also generated due to tectonic stress at Eastern California Shear Zone and witnessed of several aftershocks (Nanjo, 2020). Ide et al. (2018) discovered that tidal stress has a significant impact on the formation of earthquake hotspot zones, with the likelihood of an earthquake increasing during high tidal stress. With increasing tidal load, tectonic tremor increased at an exponential rate (Houston, 2015). According to Ide et al. (2016), large well-known earthquakes such as the Sumatran earthquake in 2004, the Maule earthquake in Chile in 2010, and the Tohoku-Oki earthquake in Japan in 2011 all had a similar tendency to occur at times of high tidal stress amplitude and decreased Gutenberg-Richter b value. There is an inverse link between stress and the Gutenberg-Richter b value (Ide et al., 2016; Schorlemmer et al., 2005). This b value is significant in measuring aftershocks in earthquake-prone areas; if the b value is increased, there is a low probability of aftershocks, whereas a dramatic reduction in the b value is connected with a greater possibility of aftershock (Vishnu and Srinu, 2014). In magnitude frequency distribution along the major strike fault of southern California, Steven and Wesnouky (1994) employed the characteristic distribution model rather than the Gutenberg-Richter relation. Most earthquake-induced areas have seen recurrence intervals of several hundred years after the first occurrence of the earthquake (Molnar, 1979); Northeast China (Lee et al., 1976) and Turkey (Ambraseys, 1971) have also experienced similar aftershocks after several hundred years. The release of seismic energy causes earthquakes to reoccur on a regular basis (Fischer and Horálek, 2003); this swarm-like aspect of seismicity is evident in the NW Bohemia region at the Novy Kostel major focal zone (1985–2001) and the New Madrid earthquake (1811–1812). Usually in this case, the region, instead of being under stress for a long duration and preparing itself for a large magnitude earthquake, releases strain energy instantaneously through such small magnitude earthquakes. A few places in the Indian shield area have previously witnessed swarm-type earthquakes, These events were attributed to triggering rainfall during the monsoon season (Singh and Mishra, 2015). Similarly, Sikkim Himalayan region is notably characterized with intense micro seismic activity region (Chowdhuri et al., 2022a, 2022b; Pal et al., 2008; Varo et al., 2019a, 2019b). Volcanism is accompanied with swarm characteristics in Mid Atlantic Ridge (Bergman and Solomon, 1990a). Micro earthquake and swarm like nature in Mid Atlantic Ridge also accompanied with volcanism. The Indian Ocean earthquake in 2012 triggered the several remote aftershocks worldwide consist with love wave radiation from main shock (Pollitz et al., 2012). Because of its underlying plate dynamicity, the Pacific Ring of Fire is the most susceptible area on the planet, resulting in the deadliest earthquakes and Tsunami. Arica earthquake and tsunami in Chile in 1868, Shanriku earthquake and tsunami in Japan (1896, M_W ~8.5), San Francisco earthquake and tsunami in USA (1906, M_W ~8), Great Kanto earthquake in Japan (1923, M_W ~7.9), Unimak Island earthquake in USA (1946, M_W ~8.1), Chilean earthquake (1960, M_W ~9.5), Anchorage earthquake (1964, M_W ~9.2), Guatemala earthquake (1976, M_W ~7.5), Tangshan earthquake in China (1976, M_W ~7.5), Indian Ocean earthquake and tsunami (2004, M_W ~9) and New Zealand earthquake (2011, M_W ~6.3) were the major notorious earthquakes of 20^{th} century along the Pacific rim, which resulted huge geologic and geomorphic change in earth surface quite a lot of times and caused great suffering in life forms (Rathore, 2003). Several scholars (Silva et al., 2006; Weischet and Huene, 1963) have discovered a link between geomorphologic alterations in SE Spain and the Chile (May, 1960) earthquake. As a natural event, earthquakes appear abruptly, causing a devastating result that may end in massive casualties (Adams, 1990). More than millions of earthquakes are recorded worldwide at seismic stations, some of which are felt by us due to their great intensity and shallow depth placement (Doocy et al., 2013). The focal depth of an earthquake is typically 700 km beneath the surface, and the intensity of shaking reduces with increasing distance from the source of the earthquake (US Geological survey, 2009). In general, the area of the oceanic ridge and subduction zone is connected with shallow and deep focal earthquake sources.

Earthquake magnitude is measured using the Richter scale, which is based on the logarithmic scale concept, which means that M_W of 6 earthquakes is approximately 10 times stronger than M_W of 5 earthquakes and 100 times stronger than M_W of 4 earthquakes. This value is based on the total radiated seismic energy by the earthquake (Chung and Bernreuter, 1981). The M_W >7.0 may be responsible for extensive destruction whereas M_W with 2.5 is not felt by human beings (Doocy et al., 2013). The modified Mercalli scale is also used to assess the impact of an earthquake, consisting of class I (no damage) to XII (complete destruction) on the basis of the severity of the damage. The tremendous intensity of the earthquake is a scourge to the life of those who live through it. It also causes certain potentially fatal threats, such as a tsunami, landslide, mudslide, fire, and flood. According to US Geological Survey (USGS) couple of earthquakes with varying magnitudes, 30 (M_W ~above 8); 434 (M_W ~7–7.9); 4220 (M_W ~6–6.9) and 46721 (M_W ~5–5.9) have recorded worldwide with 923463 death tolls and huge property loss from 1990-2020 time period. Seismology has made numerous attempts to mitigate this type of hazardous condition (Kanamori et al., 1997). Sekac et al. (2016) have employed the micro hazard zonation approach in small area earthquake studies, which plays a noteworthy role in small scale hazard zonation mapping. Artificial intelligence-based real-time focal depth identification and rapid magnitude level estimation play a critical role in determining the aftershock pattern and instantaneous damage (Kuang et al., 2021). Many regions experienced foreshocks of earthquakes (Jones and Molnar, 1976), and Bouchon et al. (2013) established that inter-plate earthquake zones preceded high foreshocks sequence compare to intra-plate zones; it can help to mitigate the earthquake risk at the plate boundaries. Land surface temperature variations caused by stress actions in tectonically active zones might also give key indicators of future earthquake potential (Choudhury et al., 2006); the related area of the Bam earthquake in southeast Iran (2003, $M_w \sim 6.6$) and the Dahoeieh-Zarand earthquake in central Iran (2005, $M_w \sim 6.0$) had short-term surface temperature anomalies ranging from 5-10°C prior to earthquake occurrence. Earthquakes are the most severe natural phenomena that have a negative impact on human lives. All prediction measurements and natural indicators of tectonic activity can aid in the identification of global earthquake hotspot and coldspot regions.

In this study, we focused on identifying earthquake hotspot and coldspot zones using 7773 historical earthquake data of three M_w classes (4.5, 4.5–6.0, and >6.0) across the world's plate boundary. (Jana et al., 2019; Pal et al., 2018; Sekac et al., 2016a, 2016b; Varo et al., 2019a, 2019b) have drawn the implication of geomatic technique significantly in natural hazard study also got the superior result. Henceforth, the geospatial approach become more efficient in earthquake prediction studies; thus, several researchers (Sekac et al., 2020, 2016c) have successfully applied this approach to earthquake susceptibility zone prediction. Therefore, in our present study, we have employed two statistical methods, hotspot analysis (Getis-Ord GI*) and optimized hotspot analysis to identify global earthquake hotspot and coldspot zones using a geographic information system (GIS) platform. Henceforth, Hotspot and coldspot zones are identified at 99%, 95%, and 90% confidence levels.

1.1. Paradigm and tectonic evidence

Whereas a tectonic event is a physical occurrence resulting from the movement of the earth's crust and predominately causes the formation of earthquakes and volcanic eruptions. Most particularly, plate tectonics can be defined as the horizontal movement of lithosphere plates over the mantle. Divergent plate boundaries form through sea-floor spreading (Le Pichon, 1968), at transform plate boundaries through strike-slip faulting (Woodcock, 1986), and convergence plate boundaries through the subduction process (Parsons et al., 2020). The phenomenon of plate tectonics on the planet earth is unique from the rest of the solar system (Kasting and Catling, 2003), although the mechanism behind this activity i.e. mantle convection is still mostly unresolved (Bercovici et al., 2015). In this perspective, several questions arise among the researchers, among them the most important one is conditions under plate tectonics takes place (Korenaga, 2020). In this regard, different supporting evidence of plate tectonics have emerged like Wilson Cycle (Wan et al., 2020) and independent plate rotation and motion theory (Brenner et al., 2020).

In 1960s, the idea of plate tectonics has been accepted by most of scientists across the world. This is due to the reliable description of the performance of the earth's lithosphere that was formulated in this time period (Palin and Santosh, 2020). It is also mentioned here that the paradigm of plate tectonics began many years back. In the late 16th century several explorers like Sir Francis Bacon have been notified that the coastlines of both sides of the Atlantic Ocean are similar in shape. Later on, in the 18th and 19th centuries, several philosophers and naturalists like Alexander Von Humboldt and Theodor Christoph Lilienthal have been found geologic and geometric similarities along both the coastlines (Kearey et al., 2009). In 1910, F. G. Taylor, firstly applied the idea of a 'drifting' landmass based on the concept of 'uniformitarianism'. Later on Taylor's drifting hypothesis resembles now to the continental drift (Le Grand, 1988). In 1912, Professor Alfred Wegener, a German scholar presented the concept of horizontal continental motion i.e. drifting of the continents, although seeds of the continental drift theory were implemented in his mind during his first expedition to Greenland in 1906-1908 (Wegener, 1912). There are several views in favor of this continental drift theory such as continuity of geological structure along the Cape fold belt, stratigraphic sequences, palaeomagnetic evidence, evidence of Permian-Carboniferous glaciations, fossil of fauna and flora along the shorelines of South America and Africa, and building of young fold mountains along the frontal edges of North and South America (Piper et al., 1973). In the Carboniferous period, all the continental landmasses were closely aggregated and formed one supercontinent which Wegener termed Pangaea meaning 'all the earth'. Later on, this assembly of continental land masses had broken apart into two parts namely Gondwanaland (Africa, South America, Antarctica, Australia, and Peninsular India) and Laurasia (North America, Europe, Greenland, and Asia; Olsen, 1997). The two supercontinents of Gondwanaland and Laurasia were separated by a wide belt of a shallow sea called the Tethys sea and surrounded by a vast ocean called Panthalasa that was the proto- Mediterranean Sea and proto-Pacific ocean respectively (Arias, 2008). Afterward, the discovery of convection current in the mantle by Holmes (1928) due to the heat of radioactive decay may cause for drifting of the continents across the Earth's surface. In the 1940s and 1950s, the development of paleomagnetism and radiometric dating indicates that the position and orientation of magnetic poles in many continental rocks differ from the present time period which also proved that continents are not always in the same position (Collinson and Runcorn, 1960). In 1962, Harry Hess developed his sea floor spreading theory based on his studies of 'Mid-ocean ridge' maps which were prepared during and after the World War II, and revealed that new ocean crust was developed at mid-ocean ridge and spread out due to pushing the continents apart (Hess et al., 1962). Afterward the development of transform faults research study revealed that the earth surface consist by seven major and numerous smaller plates which formed complex mosaic earth crust and arrange like a jigsaw pattern (Wilson, 1965). It is also mentioned here that the term 'plate' was first used by Tuzo J. Wilson in 1965 when he defined transforms faults, and it came into general in 1968 after Euler's theorem was applied to the study of movements along transform faults (Wilson, 1968). The paradigm of plate tectonics concept was widely accepted among the prominent geoscientist in 1969 at the Geological Society of America Penrose Conference, Pacific Grove, California.

1.2. Historical earthquake evidence

A number of significant earthquakes have occurred in the historical time periods. They do not have any routine instrumental recording rather their evidence is mainly found in written record sources. Therefore, there is significant uncertainty regarding the sources, magnitude, and date of historical earthquakes. It is also mentioned here that the number of fatalities is also often very uncertain, particularly for the older major earthquake events. The Chinese philosopher Chang Heng in A.D. 132 invented the earliest seismoscope which was used to measure the earthquake. This seismoscope was consisting by eight dragon heads facing the eight principal directions of the compass (Dewey and Byerly, 1979). In 1926, Harold Jeffreys was the first to claim scientifically regarding the earthquake based on his study of earthquake waves (Cook, 1990). The scientific study of earthquakes is comparatively new and elaborately described the causes and optimal consequences. Scientists have divided the occurrences of historical earthquakes into four groups such as pre-11th century, 11th–18th century, 19th century and 20th century earthquakes. In the prehistoric time period China, Greece, Iran, Turkey, Syria, Japan, and Armenia have faced frequent earthquakes (List of historical earthquakes, 2021). The descriptive information of the earliest earthquake occurred in China in 1177 B.C. In Europe, the earthquake is mentioned near about 540 B.C. In America, the earliest known earthquakes were in Mexico (late 14th century) and Peru (1471). Although the description of all these earthquakes is not well documented. The effects of earthquakes around the globe were published by the end of the 17th century. The first recorded evidence of an earthquake has been traced back to 1831 B.C. in the Shandong province of China. Hence, there is a fairly complete record starting in 780 B.C. during the Zhou Dynasty in China. The most widely felt earthquakes in North America were a series that occurred in 1811–1812 (December 16, 1811; January 23, 1812; February 7, 1812) near New Madrid, Missouri, with an estimated magnitude near about 8 M_W. Alongside, the San Francisco earthquake of 1906 was one of the most destructive in the recorded history of North America. In the southwest of Guadalajara, Mexico, a large earthquake occurred on 27th December 1568 (Suárez et al., 1994). The historical reports indicate that the 1568 earthquake was the largest earthquake in the Trans-Mexican volcanic. Studies also reveal that in the volcanic belt large earthquakes occurred in 1875, 1912, and 1920 with magnitudes near about and greater than M_W 7.0 (Suárez et al., 1994). In the Kythira strait, Greece, more than ten large earthquakes (M_W >6.0) occurred from 1750 to 1910 (Papadopoulos and Vassilopoulou, 2001). In Japan, a giant earthquake (M_W 9, estimated from the tsunami height) was noticed on 26th January 1700, which ruptured the whole length of the Cascadia subduction zone (Satake et al., 1996). The major earthquakes phenomenon of the world has occurred in the subduction zone of plate boundaries with high magnitude. In the recent historical past, the ten biggest earthquakes occurred across the world with respective magnitudes are as in Ecuador coast, 31 January, 1906 (M_W 8.8), Assam, Tibet, 15 August 1950 (M_W 8.6), Kamchatka, Russia, 4 November, 1952 (M_W 9.0), Valdivia, Chile, 22 May, 1960 (M_W 9.5), Prince William Sound, Alaska, 28 March 1964 (M_W 9.2), Rat Islands, Alaska, 2 April 1965 (M_W 8.7), Sumatra, Indonesia, 26 December 2004 (M_W 9.1), Sumatra, Indonesia, 28 March 2005 (M_W 8.6), Biobio, Chile, 27 February 2010 (M_W 8.8) and Sendai, Japan, 11 March 2011 (M_W 9.0). In the last few decades, seismologists have noticed an increase in high-magnitude and high-impact earthquakes in the world's most earthquake prone areas. Scientists reveal that it is due to the energy released by earthquakes on a global scale in the last decade is much more than in the previous 25-30 years.

2. Materials and methods

2.1. Database

The development of a reliable earthquake hotspot and coldspot map of the entire world and its precession level remarkably depends on the availability and size of the datasets using an appropriate modeling approach. Hence, a large dataset can help in enhancing the performance level as well as support to make greater experimental output in all adopted modeling approaches. Apart from this, the records of worldwide earthquake zones have a significant influence on probable earthquake hotspot and coldspot zones making up the entire world. Thus, the larger datasets are a prime concern in any natural hazard study. Therefore, in our current study, a total of 7773 historical earthquake epicenter points were collected to analyze the earthquake hotspot and coldspot zone from the USGS earthquake catalog (https://earthquake.usgs.gov). The magnitude of the collected earthquake epicenter points was divided into three categories i.e., below 4.5, 4.5 to 6.0 and above 6.0 (Fig. 1).

2.2. Methodology

Although, a precise earthquake hotspot and coldspot map and their degree of accuracy are defined by the size of the datasets but also depend on a suitable modeling approach. The appropriate model with a proper methodological framework for the appropriate study region is essential to develop the exact hotspot and coldspot zone. Henceforth, the following steps have been carried out in the present study to fulfill our research objectives (Fig. 2):

- Historical earthquake data were collected as input parameters in this study.
- Statistical methods of hotspot analysis and optimized hotspot analysis were used to identification of hotspot and coldspot zones using ArcGIS 10.5 platform.

2.2.1. Statistical analysis

In this study, hotspot analysis and optimized hotspot analysis methods were used to identification of earthquakes hotspot and coldspot. The basic difference between the hotspot analysis and optimized hotspot analysis is that hotspot gives more control over the selected parameters, whereas the optimized hotspot tries to make some smart choices for some of the selected parameters. The selected two methods are described in the following section:

2.2.2. Hotspot analysis

A hotspot is defined as a particular small area or location that denotes the deliberation of incidents within a well-known boundary (Prasannakumar et al., 2011). Three processes namely events collection, clusters mapping by Getis-Ord GI* function, and estimation of density through kernel density tool are involved in hotspot analysis (Jana and Sar, 2016). In this research study, Getis-Ord GI* statistic method was used for the identification of hotspot and cold spot cluster mapping of an earthquake based on a fixed distance band in ArcGIS 10.5 software. The method of G-statistics, proposed by Getis and Ord (1992) was used for spatial pattern analysis as an evidence tool. The high and low values of a spatial cluster represent through the result of the Z score, in which hotspots are indicated through positive or higher values of the Z score, i.e., clustering of high values and cold spot represents through negative or small values of the Z score, and whereas no spatial clustering is indicating through Z score of near-zero values (Manepalli et al., 2011). The hotspot analysis of Getis-Ord GI* statistics can be expressed as:

$$G_i^* = \frac{\sum_{j=1}^{n} w_{i,j}x_j - X^- \sum_{j=1}^{n} w_{i,j}}{s\sqrt{\frac{\left[n\sum_{j=1}^{n} w_{i,j}^2 - \left(\sum_{j=1}^{n} w_{i,j}^2\right)\right]}{n-1}}} \tag{1}$$

where, x_j express the attribute value for feature j, $w_{i,j}$ represent the spatial weight between feature i *and* j, and n represent the total number of features, and:

$$X^- = \frac{\sum_{j=1}^{n} x_j}{n} \tag{2}$$

$$S = \sqrt{\frac{\sum_{j=1}^{n} x_j^2}{n} - (X^-)^2} \tag{3}$$

2.2.3. Optimized hotspot analysis

Optimized hotspot analysis is executed based on a hotspot analysis tool using input parameters dataset. Optimized hotspot analysis tool interrogates input data to gain the settings from the

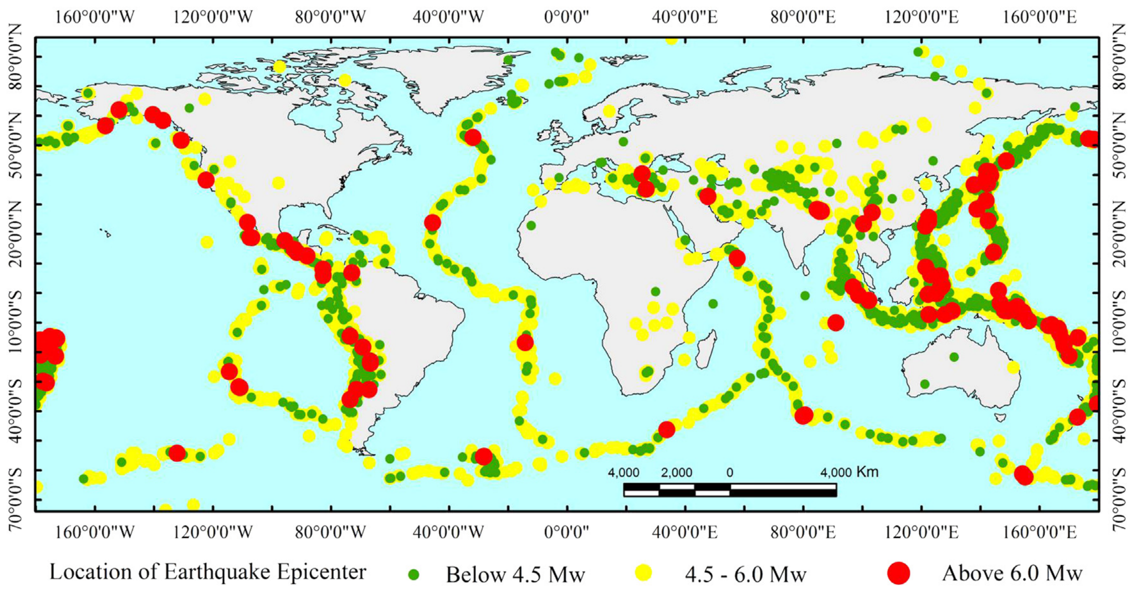

Fig. 1. Location of the earthquake epicentres with its moment magnitude (M_w) values. Source: USGS earthquake catalogue.

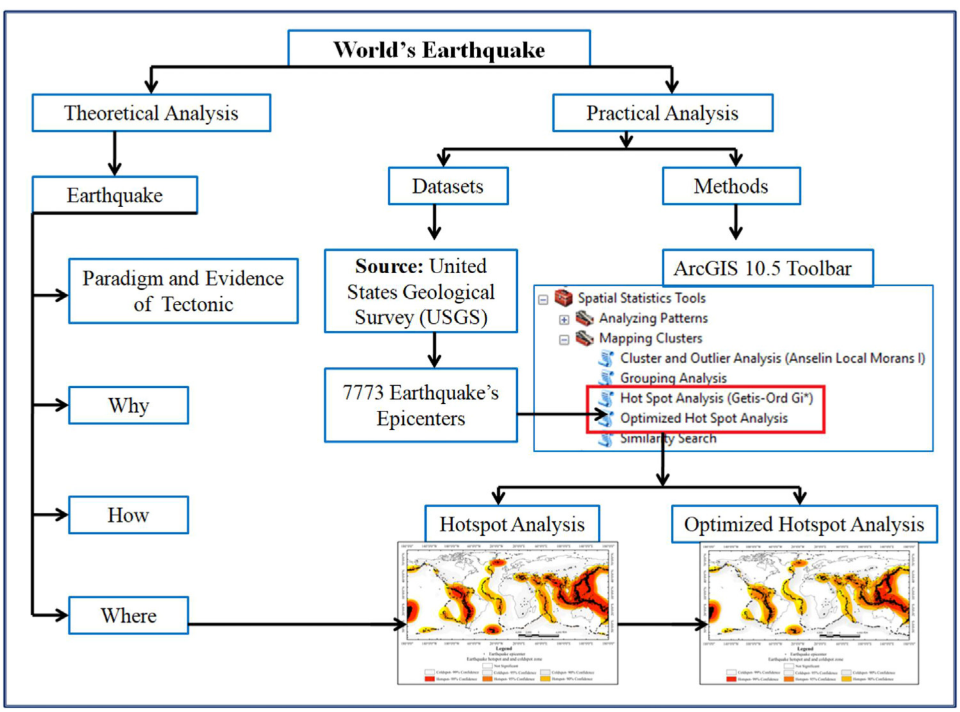

Fig. 2. Methodological flow chart of this study. Earthquake hotspot and coldspot points were derived from the USGS earthquake catalogue.

result of hotspot analysis. In optimized hotspot analysis, if the input attributes dataset contains incident of point data then this tool will aggregate this point data into the weighted feature. The optimized hotspot analysis tool will recognize an appropriate scale of analysis using the distribution of weighted features. It is just like a function of a camera, i.e., camera has a manual function that allows overriding the automatic settings, and the Getis-Ord Gi* based hotspot analysis tool allows full control over all input parameters. Using an Optimized hotspot analysis tool with the function of noting the parameter settings may help to process the parameter and providing to full control of the hotspot analysis tool. The details about the optimized hotspot analysis and how it is work may find in https://desktop.arcgis.com/en/arcmap/10.7/tools/spatial-statistics-toolbox/how-optimized-hot-spot-analysis-works.htm.

3. Results

3.1. Where?

The epicenter of earthquakes occurs mostly along the tectonic plate boundary, more frequently on the 'ring of fire'. In this study, hotspot analysis and optimized hotspot analysis methods were applied to identify the world's earthquake hotspot and coldspot zone

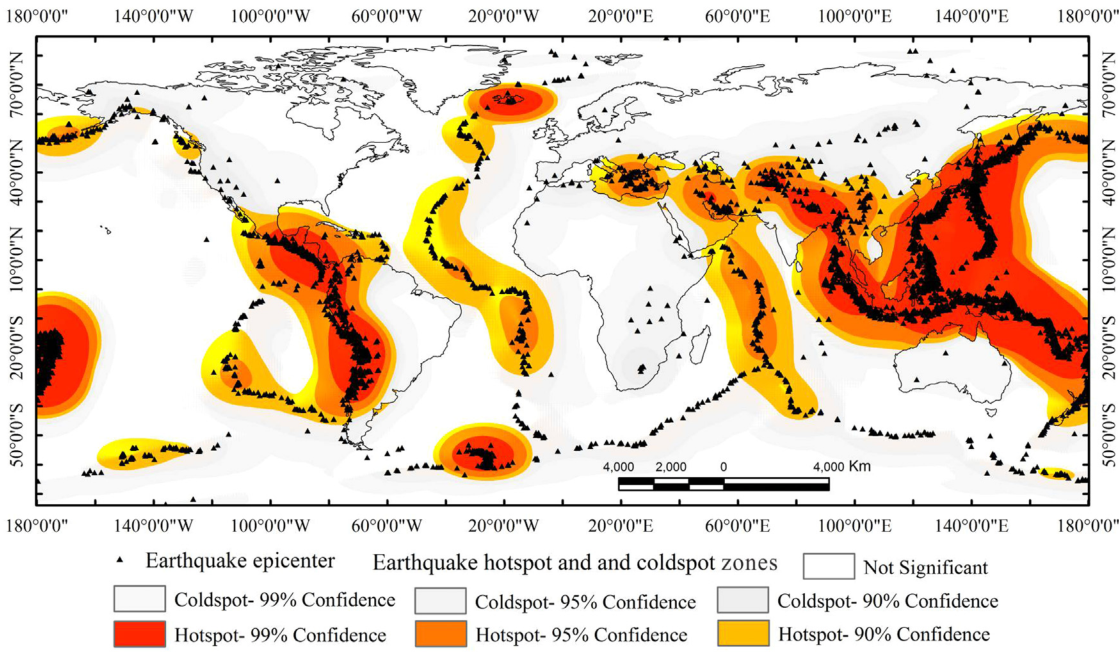

Fig. 3. Earthquake hotspot and coldspot zone based on hotspot analysis (Getis-Ord Gi*). Source: USGS earthquake catalogue.

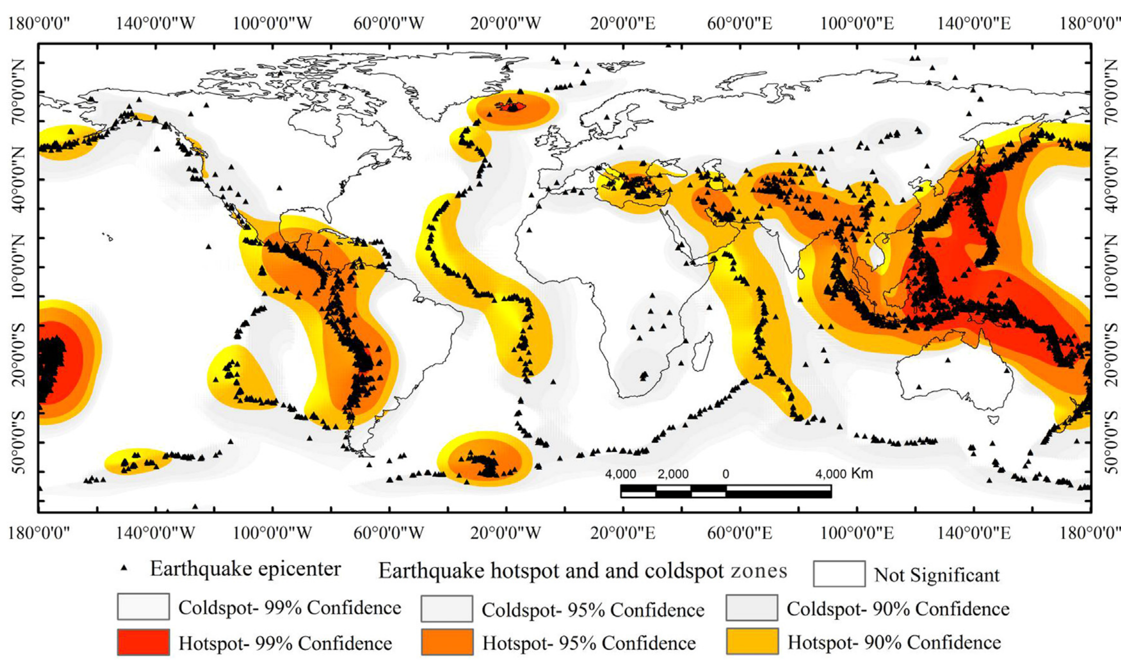

Fig. 4. Earthquake hotspot and coldspot zone based on optimized hotspot analysis. Source: USGS earthquake catalogue.

and the outcome result is presented in Figs. 3 and 4, respectively. Both the earthquake hotspot and coldspot maps indicate that hotspot zones are found along the tectonic plate boundaries and their surrounding areas. In the hotspot analysis map, major hotspot areas of 99%, 95%, and 90% confidence levels are found along the pacific ring of fire, mid-Atlantic oceanic ridge, and Peru-Chile Trench, in the Mediterranean region, and Indian ocean ridge. In the case of optimized hotspot analysis, a hotspot zone at 99% confidence level is found along the pacific ring of fire and the northern part of mid-Atlantic oceanic ridge, and a hotspot zone at 95% and 90% confidence level is found along the Peru-Chile Trench, mid-Atlantic oceanic ridge, Indian oceanic ridge and some isolated areas. The result of hotspot analysis (Getis-Ord Gi*) indicates that the hotspot zone of the world is occupied by 5.53%, 6.04% and 6.49% at 99%, 95%, and 90% confidence levels respectively, and the coldspot zone of the world is occupied by 37.53%, 28.75% and 7.16% at 99%, 95%, and 90% confidence level respectively. On the other hand, the result of optimized hotspot analysis indicates that the hotspot zone of the world is occupied by 2.27%, 5.19% and 4.56% at 99%, 95%, and 90% confidence levels respectively, and the coldspot zone of the world is occupied by 51.39%, 9.91% and 9.75% at 99%, 95% and 90% confidence level respectively.

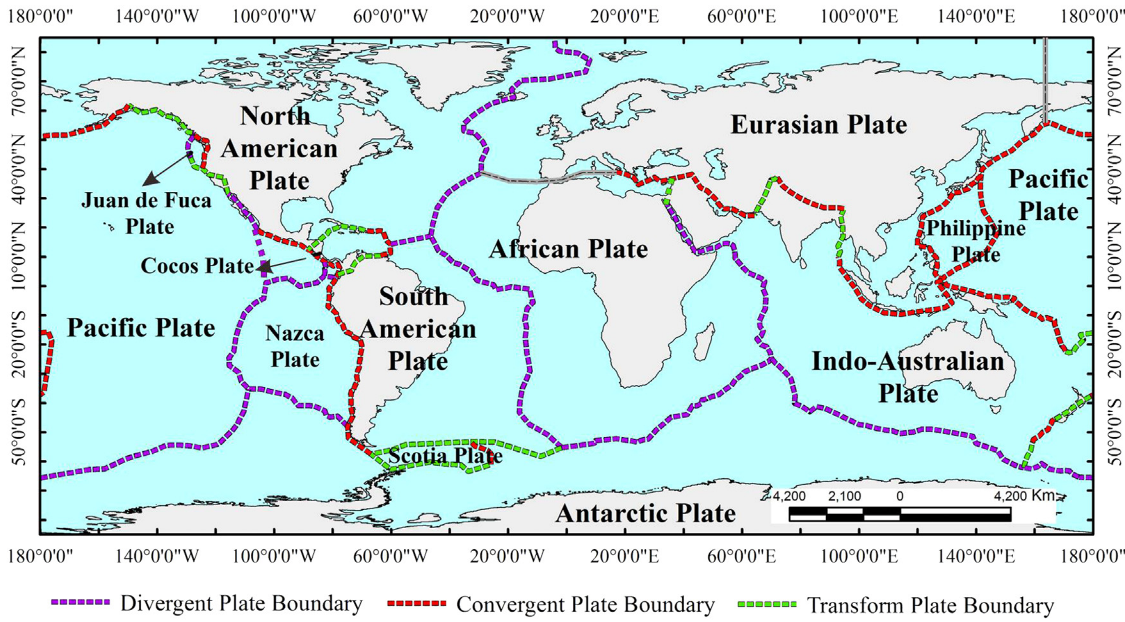

Fig. 5. Major plates and three types of the plate boundary zone to show the hotspot and coldspot locations.

The occurrences of earthquakes in this area are due to the cause of plate subduction, collision and transformation along with each other.

3.2. Why?

The earth's lithospheric surface consists of several major and minor plates and three types of plate boundaries are found among them and they are namely divergent, convergent, and transform plate boundaries (Fig. 5). These plates are not in a stable form rather they move from each other in their own direction with a defined rate and the rate of movement is differ considerably from one to another. These movements of the plate are responsible for the occurrence of earthquakes of the world and this phenomenon is found particularly along the narrow belt of plate boundaries. This is due to the sudden release of energy by the collision of two plates or subduction of the denser or heavier plate under the lighter plate. This collision-induced energy hit the Earth's lithosphere that creating seismic waves and shaking the surface of the Earth at a different magnitude of rate. This seismicity has occurred in the mid-oceanic ridges, trench arc zone, major fracture zones, and young orogenic belts. All of these features are located in the plate boundaries where plate subduction or collision among each other is responsible for this kind of devastating phenomenon. The oceanic lithosphere (denser and heavier) descends into the continental lithosphere or lower denser oceanic plate at subduction zones and strain energy is released which generates earthquakes. This subduction activity is found along the Tonga region of the South Pacific ocean where the lithosphere moves downwards at an angle of about 45°. The formation of the earthquake in the subduction zone is often called Benioff zones. The Benioff zone earthquakes are formed in several places all over the world among them central Aleutians, Hindu-Kush-Pamir region, and Wadati Benioff zone are more devastating. Therefore subduction zones are sites of the most intense and widespread occurrences of earthquakes. The most fundamental concept regarding the origin of earthquakes is that plates interact with each other along their margins, therefore strain is built up and suddenly rupture generating seismic activity along this boundary. Thus, most of the earthquake epicenters are located along with the narrow bands of oceanic ridges, transforming fault, and Benioff/subduction zones. The origin of the location of seismicity varies according to the position of plate boundaries and their rate of subduction, which may be classified as shallow focus (less than 70 km), mid focus (70 to 300 km), and deep-focus (300 to 700 km) earthquakes. Alongside, convergent plate boundary or divergent plate margin is also responsible for occurrences of earthquakes and volcanos due to the advancing continental plate overriding the oceanic plate. Therefore volcanos and earthquakes are associated in the subduction zone like in the Andes due to the subduction of the Nazca plate under the South American plate, similarly, Pacific plate subduction causes volcanoes and earthquakes in Bering, Kamchatka, Japan, Philippines, and New Zeland. The subduction of the Indian plate occurs earthquakes in Java, Sumatra, and Bali. It is also mentioned here that the collision of the Indian plate and Eurasian plate was also responsible for the devastating earthquake in the Himalayan and its surrounding regions.

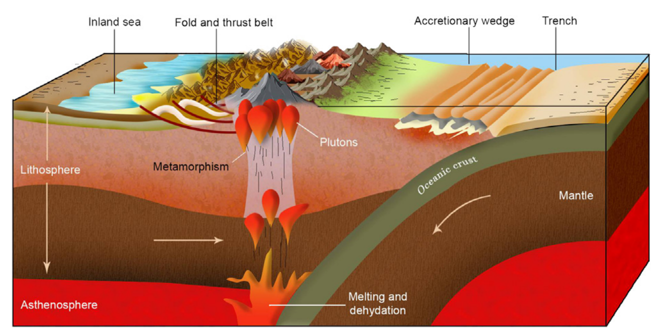

Fig. 6. Movement of lithospheric plates due to the presence of asthenosphere and conventional current force in the upper mantle region after Holmes (1931).

3.3. How?

The broad regime of tectonic activities may occur in the interior of the earth and these tectonic events are responsible for the occurrences of earthquakes, volcanoes, and another related phenomenon (Figs. 6 and 9). The lithosphere is differentiating from the underlying asthenosphere and the lithospheric plates move due

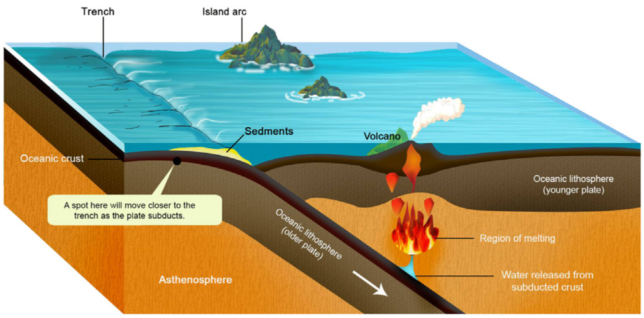

Fig. 7. Rising of mantle rock in the form of lava at the mid-oceanic ridge (oceanic-oceanic plate collision) and sinking rocks has been taken place beneath island and mountain arcs after Morgan (1968).

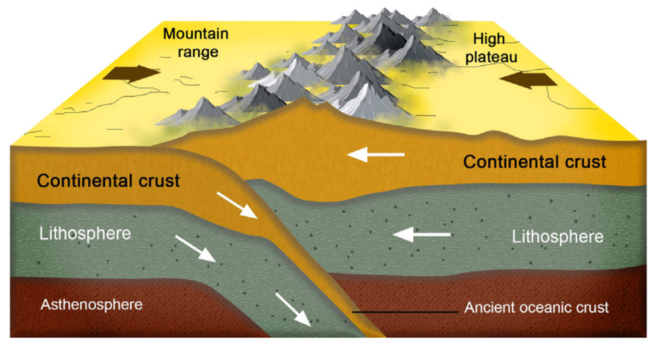

Fig. 8. Collision occurs among the two plates (continental-continental) and subduction takes place. Significant earthquakes have taken place at this region (Morgan, 1968).

to the presence of this asthenosphere layer. More specifically, the plate moves in a substantial horizontal motion concerning the underlying asthenosphere with an average relative velocity of 0.8–1.8. Several geologists and geoscientists have hypothesized that the horizontal motion of tectonic plates is related to the convection currents in the earth's mantle. The convection currents describe the rising, spread, and sinking of gas, liquid, or molten material caused by the sufficient heat in the earth's interior. Majority of the scientist believe that the thermal convection currents come from great depth in the mantle. It is fact that this current is caused by differential heating of mantle rocks and it is also responsible for differences in rock density. Thus, higher temperature rock becomes lighter and has less dense than those of lower temperature and higher density. Therefore, a cycle of rising and sinking rocks motion is noticed in the mantle, and simultaneously convection currents are formed. This convectional cycle causes the rising of mantle rock at the mid-oceanic ridge and sinking rocks has been taken place beneath islands and mountain arcs (Fig. 7). Thus, the new molten rock material from the mantle reaches the mid-oceanic ridge and forms younger rock, on the other side older lithosphere moves apart from the mid-oceanic ridge and descends to the subduction zones. In this way plates move from each other and collision or subduction among them causes occurrences of earthquakes. Depending upon the direction of movement of the plates three main types of plate boundary are recognized. Which constructive plate boundary is the area where plates are drifting away and it is characterized by the upwelling of the molten lava and the formation of new oceanic crust. The mid-Atlantic ridge is a typical example of this type of boundary where the American plate and Eurasian African plates move in the opposite directions. In the destructive plate boundary, two lithospheric plates move towards each other and a collision takes place. The plane in which collision occurs among the two plates and subduction takes place is called the subduction zone (Fig. 8). The Peru-Chile Trench is such a type of the plate boundary in which the Nazca plate is plunging under the South American plate. The transform plate boundary is the zone where two adjacent lithospheric plates slip horizontally and, in this zone, crust is neither created nor destroyed. The San Andreas Fault is such type of plate boundary where the Pacific and North American plate is on the west and east side of the fault respectively. The transform boundaries are characterized by occurrences of numerous earthquakes.

4. Discussion

The earth's surfaces vary with continents and ocean basins, and such complex elements, many of which have past accidental shapes, would not be possible to mathematically estimate. Seismic regimes have a high potential for generating large earthquakes, resulting in massive loss of life and severe infrastructure damage.

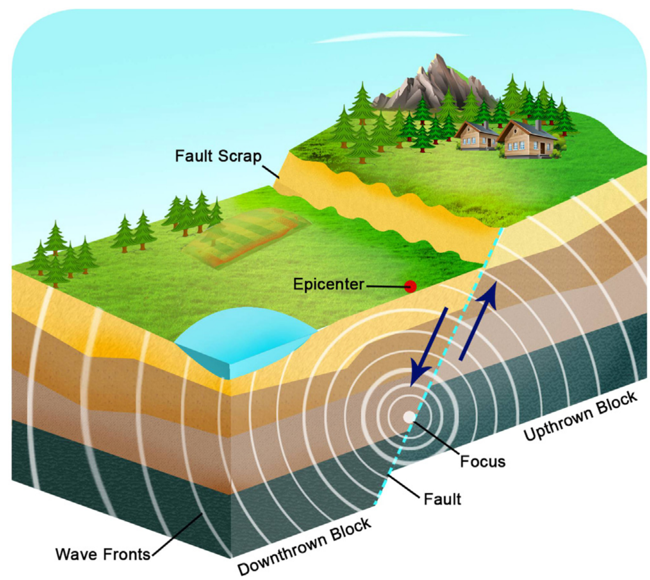

Fig. 9. The distinct plate movements and helps to occur earthquake events.

In modern seismology, earthquake zonation is the most complicated and critical problem, and it is desperately needed on a global scale. In this study, we used hotspot (Getis-Ord GI*) and optimized hotspot analyses in a GIS platform to determine the global hotspot and coldspot of earthquakes. The aforementioned methods show a notable earthquake pattern throughout the world especially in the active plate movement region; this continuous and connected pattern of earthquake hotspot regions is the evidence of global large plate movement in a sequential direction. Therefore, the results displayed that the Pacific ring of fire (Aleutian Island, Kamchatka peninsula, Japan, Philippines, Sumatra, Tonga, North Island, New Zealand, Mexico, Andes region, etc.) the mid-Atlantic ridge (central part), the Peru-Chile Trench, the Indian Ocean ridge (Sunda Arc, Andaman-Nicobar Arc, Makran region), and the Mediterranean region (Italy, Greece, Turkey) are all extremely vulnerable to earthquakes due to significant plate movements. Previous studies, such as those (Paton and Jang, 2016), show that 90% of the world's earthquakes occur in the circum-pacific belt; The ring of fire as the part of the circum-pacific belt is one of the significant geologically active areas in the world comprises with frequent earthquakes with the association of devastating volcanoes and also has evidence of around 81% global largest earthquakes in the ring of fire region (Masum and Akbar, 2019). Eggert and Walter (2009), Olson (1989) and Parwanto and Oyama (2014) present historical evidence, and statistical analysis, and make a connection between volcanic activity, geothermal energy, and tsunami with earthquakes in the Pacific Ring of Fire. Kanamori and Stewart (1976) and Bohnenstiehl et al. (2003) observed the intensity and spreading behavior of seismicity at the Mid-Atlantic ridge; Several researchers (Bergman and Solomon, 1990b; Oliveira and Lin, 2019; Smith et al., 2003) successfully established and make significant research work on Mid Atlantic ridge earthquake and got noteworthy evidence and reasons of earthquake occurrences. Swift and Carr (1974), Kahle et al. (1998) and McCloskey et al. (2008) investigated the potentiality and future probability of earthquakes in the Peru-Chile Trench, Indian Ocean ridge, and Mediterranean region. Indian Ocean basin has remarkable data about hazardous earthquake scenarios such as the 2004 earthquake-induced Tsunami (Okal and Synolakis, 2008) earthquake at Sunda, Makran region (Jaiswal et al., 2008). As a result, our findings on the global hotspot and coldspot earthquake areas are very similar to previous research work. The findings of this study show that hotspot (Getis-Ord GI*) and optimized hotspot analyses are directly relevant to predicted earthquake potential areas on Earth. Hotspot studies offer a wide range of scientific and environmental applications due to their intensive spatial and temporal sampling of earthquake sites and magnitudes in the oceans and along their margins. We have provided records relating to major and minor earthquakes on a worldwide scale in this article. The approach varies from previous research in that it uses hotspot analysis rather than another statistical model for conditional earthquake hotspot mapping. To demonstrate, we compared the method proposed in this research to optimized hotspot analysis methodologies of the probability for earthquake hotspots based on the Getis-Ord GI* of the hotspot studies. The comparison of the obtained results for several previous prominent earthquake sequences indicates that the method based on the Getis-Ord Gi* based hotspot analysis and the cluster estimates of the model parameters provides typically higher probabilities for the occurrence of the expected earthquake than the methods based on the spatial cluster represented through the result of the Z score distribution.

5. Conclusions

We investigated various seismological hotspot and coldspot areas around the world using historical data. We discovered a significant clustering of seismic activity in areas with frequent plate movements. The aforementioned hotspot analysis (Getis-Ord GI*) result specifies worldwide occupied hotspot areas (37.53%, 28.75%, and 7.16%) at 99%, 95%, and 90% confidence levels respectively. Alternatively, optimized hotspot analysis specifies occupied hotspot areas (2.27%, 5.19%, and 4.56%) and coldspot areas (51.39%, 9.91%, and 9.75%) at 99%, 95% and 90% confidence level respectively. The results show that the Pacific ring of fire (Aleutian Island, East Asian countries, Philippines, South America, Central America, and North America), Peru-Chile Trench also known as the Atacama Trench, mid-Atlantic oceanic ridge, and the Indian ocean ridge (Sunda region, Makran region, Andaman Nicobar belt) are all significantly vulnerable to earthquakes and are located in hotspot zones with 99%, 95%, and 90% confidence levels, respectively. Although, this study has a crucial role in global earthquake distribution studies and findings of worldwide earthquake potential areas, our research has some limitations. Firstly, the datasets of this study were fully collected from a secondary data source and therefore we are unable to verify this large worldwide data; secondly, due to the vastness of this data this study fully ignored the ground truth verification; thus, this study apparently verified by the secondary historical data source. Apart from these limitations, this study has worldwide implications in earthquake studies with the help of the adopted modeling approach. When the results of the two methods are compared, optimized hotspot analysis emerges as the more probabilistic method in earthquake zonation mapping. As a result, the investigation of hotspot and coldspot areas using the aforementioned statistical method is more relevant and yields better results than previously used indices for the same purposes. As a result, this method has the potential to be a valuable tool in future research.

Declaration of Competing Interests

The authors declare that they have no known competing financial interests or personal relationships that could have appeared to influence the work reported in this paper.

CRediT authorship contribution statement

Subodh Chandra Pal: Conceptualization, Supervision, Investigation, Formal analysis, Visualization, Writing – original draft, Writing – review & editing. **Asish Saha:** Investigation, Formal analysis, Visualization, Writing – original draft, Writing – review & editing. **Indrajit Chowdhuri:** Investigation, Formal analysis, Visualization, Writing – original draft, Writing – review & editing. **Dipankar Ruidas:** Investigation, Formal analysis, Visualization, Writing – original draft, Writing – review & editing. **Rabin Chakrabortty:** Investigation, Formal analysis, Visualization, Writing – original draft, Writing – review & editing. **Paramita Roy:** Investigation, Formal analysis, Visualization, Writing – original draft, Writing – review & editing. **Manisa Shit:** Investigation, Formal analysis, Visualization, Writing – original draft, Writing – review & editing.

Acknowledgments

The authors are grateful to the Department of Geography, The University of Burdwan for providing the infrastructural facilities. We are also thankful to USGS for providing the essential data.

References

Adams, R.D., 1990. Earthquake occurrence and effects. Injury, Med. Resp. Major Dis. 21, 17–20. doi:10.1016/0020-1383(90)90146-L.
Aki, K., 1966. In: Generation and Propagation of G Waves from the Niigata Earthquake of June 16, 1964.: Part 2. Estimation of earthquake moment, released energy, and stress-strain drop from the G wave spectrum, 44. Bulletin of the Earthquake Research Institute, University of Tokyo, pp. 73–88.
Albano, M., Polcari, M., Bignami, C., Moro, M., Saroli, M., Stramondo, S., 2017. Did anthropogenic activities trigger the 3 April 2017 Mw 6.5 Botswana earthquake? Remote Sens. 9, 1028.
Ambraseys, N.N., 1971. Value of historical records of earthquakes. Nature 232, 375–379. doi:10.1038/232375a0.
Arias, C., 2008. Palaeoceanography and biogeography in the early jurassic panthalassa and tethys oceans. Gondwana Res. 14, 306–315.
Avouac, J.-P., Meng, L., Wei, S., Wang, T., Ampuero, J.-P., 2015. Lower edge of locked main himalayan thrust unzipped by the 2015 Gorkha earthquake. Nat. Geosci. 8, 708–711.
Bao, H., Ampuero, J.-P., Meng, L., Fielding, E.J., Liang, C., Milliner, C.W., Feng, T., Huang, H., 2019. Early and persistent supershear rupture of the 2018 magnitude 7.5 Palu earthquake. Nat. Geosci. 12, 200–205.
Bercovici, D., Tackley, P., Ricard, Y., 2015. 7.07-the generation of plate tectonics from mantle dynamics. In: Treatise on Geophysics. Elsevier, Oxford, pp. 271–318.
Bergman, E.A., Solomon, S.C., 1990a. Earthquake swarms on the mid-atlantic ridge: products of magmatism or extensional tectonics? J. Geophys. Res.: Solid Earth 95, 4943–4965. doi:10.1029/JB095iB04p04943.
Bergman, E.A., Solomon, S.C., 1990b. Earthquake swarms on the mid-atlantic ridge: products of magmatism or extensional tectonics? J. Geophys. Res.: Solid Earth 95, 4943–4965. doi:10.1029/JB095iB04p04943.
Bohnenstiehl, D.R., Tolstoy, M., Smith, D.K., Fox, C.G., Dziak, R.P., 2003. Time-clustering behavior of spreading-center seismicity between 15 and 35 N on the mid-atlantic ridge: observations from hydroacoustic monitoring. Phys. Earth Planet. Inter. 138, 147–161.
Bouchon, M., Durand, V., Marsan, D., Karabulut, H., Schmittbuhl, J., 2013. The long precursory phase of most large interplate earthquakes. Nat. Geosci. 6, 299–302. doi:10.1038/ngeo1770.
Bradley, K., Mallick, R., Andikagumi, H., Hubbard, J., Meilianda, E., Switzer, A., Du, N., Brocard, G., Alfian, D., Benazir, B., 2019. Earthquake-triggered 2018 Palu Valley landslides enabled by wet rice cultivation. Nat. Geosci. 12, 935–939.

Brenner, A.R., Fu, R.R., Evans, D.A., Smirnov, A.V., Trubko, R., Rose, I.R., 2020. Paleomagnetic evidence for modern-like plate motion velocities at 3.2 Ga. Sci. Adv. 6, eaaz8670.
Oliveira, C.A., Lin, T., 2019. Three-dimensional global scale underwater sound modeling: the T-phase wave propagation of a southern mid-Atlantic ridge earthquake. J. Acoust. Soc. Am. 146, 2124–2135. doi:10.1121/1.5126010.
Choudhury, S., Dasgupta, S., Saraf, A.K., Panda, S., 2006. Remote sensing observations of pre-earthquake thermal anomalies in Iran. Int. J. Remote Sens. 27, 4381–4396.
Chowdhuri, I., Pal, S.C., Janizadeh, S., Saha, A., Ahmadi, K., Chakrabortty, R., Islam, A.R.M.T., Roy, P., Shit, M., 2022a. Application of novel deep boosting framework-based earthquake induced landslide hazards prediction approach in Sikkim Himalaya. Geocarto Int. 1–27.
Chowdhuri, I., Pal, S.C., Saha, A., Chakrabortty, R., Roy, P., 2022b. Mapping of earthquake hotspot and coldspot zones for identifying potential landslide hotspot areas in the Himalayan region. Bull. Eng. Geol. Environ. 81, 1–23.
Chung, D.H., Bernreuter, D.L., 1981. Regional relationships among earthquake magnitude scales. Rev. Geophys. 19, 649–663. doi:10.1029/RG019i004p00649.
Collinson, D.W., Runcorn, S.K., 1960. Polar wandering and continental drift: evidence from paleomagnetic observations in the United States. Geol. Soc. Am. Bull. 71, 915–958.
Cook, A.H., 1990. Sir Harold Jeffreys, 2 April 1891-18 March 1989. The Royal Society, London.
DeMets, C., Gordon, R.G., Argus, D.F., Stein, S., 1990. Current plate motions. Geophys. J. Int. 101, 425–478.
Dewey, J., Byerly, P., 1979. The history of seismometry to 1900. Earthq. Inf. Bull. (USGS) 11, 64–70.
Doocy, S., Daniels, A., Packer, C., Dick, A., Kirsch, T.D., 2013. The human impact of earthquakes: a historical review of events 1980-2009 and systematic literature review. PLoS Curr. 5. doi:10.1371/currents.dis.67bd14fe457f1db0b5433a8ee20fb833, ecurrents.dis.67bd14fe457f1db0b5433-a8ee20fb833.
Eggert, S., Walter, T.R., 2009. Volcanic activity before and after large tectonic earthquakes: observations and statistical significance. Tectonophysics 471, 14–26.
Fischer, T., Horálek, J., 2003. Space-time distribution of earthquake swarms in the principal focal zone of the NW Bohemia/Vogtland seismoactive region: period 1985–2001. J. Geodyn. 35, 125–144. doi:10.1016/S0264-3707(02)00058-3.
Frankenberg, E., Sumantri, C., Thomas, D., 2020. Effects of a natural disaster on mortality risks over the longer term. Nat. Sustain. 3, 614–619.
Getis, A., ORD, J., 1992. The analysis of spatial association by use of distance statistics. Geogr. Anal. 24 (3), 189–206.
Ghanbari, E., Saberi, A.R., 2006. Comparison of mechanism of north tabriz fault and north anatolian fault with mechanism of san andres fault. The 7th International Congress on Civil Engineering, Tabriz, Iran.
Ghobarah, A., Saatcioglu, M., Nistor, I., 2006. The impact of the 26 December 2004 earthquake and tsunami on structures and infrastructure. Eng. Struct. 28, 312–326.
Gulia, L., Wiemer, S., 2010. The influence of tectonic regimes on the earthquake size distribution: a case study for Italy. Geophys. Res. Lett. 37, 1–6.
Hamblin, W.K., 1975. Earth's Dynamic Systems. Burgess Pub. Co.
Hess, H.H., Engel, A.E.J., James, H.L., Leonard, B.F., 1962. History of ocean basins.
Hill, D.P., Reasenberg, P.A., Michael, A., Arabaz, W.J., Beroza, G., Brumbaugh, D., Brune, J.N., Castro, R., Davis, S., dePolo, D., Ellsworth, W.L., Gomberg, J., Harmsen, S., House, L., Jackson, S.M., Johnston, M.J.S., Jones, L., Keller, R., Malone, S., Munguia, L., Nava, S., Pechmann, J.C., Sanford, A., Simpson, R.W., Smith, R.B., Stark, M., Stickney, M., Vidal, A., Walter, S., Wong, V., Zollweg, J., 1993. Seismicity remotely triggered by the magnitude 7.3 landers, California, earthquake. Science 260, 1617–1623. doi:10.1126/science.260.5114.1617.
Holmes, A., 1931. XVIII. Radioactivity and earth movements. Trans. Geol. Soc. Glasg. 18, 559–606. doi:10.1144/transglas.18.3.559.
Holmes, A., 1928. 1930, radioactivity and earth movements. Geol. Soc. Glasg. Trans. 18, 559–606.
Houston, H., 2015. Low friction and fault weakening revealed by rising sensitivity of tremor to tidal stress. Nat. Geosci. 8, 409–415.
Ide, S., Yabe, S., Tanaka, Y., 2016. Earthquake potential revealed by tidal influence on earthquake size–frequency statistics. Nat. Geosci. 9, 834–837. doi:10.1038/ngeo2796.
Jaiswal, R., Rastogi, B., Murty, T., 2008. Tsunamigenic sources in the Indian Ocean. Sci. Tsunami Hazards 27, 32–53.
Jana, M., Sar, N., 2016. Modeling of hotspot detection using cluster outlier analysis and Getis-Ord Gi* statistic of educational development in upper-primary level, India. Model. Earth Syst. Environ. 2, 60.
Jana, S.K., Sekac, T., Pal, D.K., 2019. Geo-spatial approach with frequency ratio method in landslide susceptibility mapping in the Busu River catchment, Papua New Guinea. Spat. Inf. Res. 27, 49–62. doi:10.1007/s41324-018-0215-x.
Jones, J., Malone, S.D., 2005. Mount hood earthquake activity: volcanic or tectonic origins? Bull.e Seismol. Soc. Am. 95, 818–832.
Jones, L., Molnar, P., 1976. Frequency of foreshocks. Nature 262, 677–679. doi:10.1038/262677a0.
Kahle, H.-G., Straub, C., Reilinger, R., McClusky, S., King, R., Hurst, K., Veis, G., Kastens, K., Cross, P., 1998. The strain rate field in the eastern Mediterranean region, estimated by repeated GPS measurements. Tectonophysics 294, 237–252.
Kanamori, H., Hauksson, E., Heaton, T., 1997. Real-time seismology and earthquake hazard mitigation. Nature 390, 461–464. doi:10.1038/37280.
Kanamori, H., Stewart, G.S., 1976. Mode of the strain release along the Gibbs fracture zone, Mid-Atlantic Ridge. Phys. Earth Planet. Inter. 11, 312–332.
Kasting, J.F., Catling, D., 2003. Evolution of a habitable planet. Annu. Rev. Astron. Astrophys. 41, 429–463.
Kearey, P., Klepeis, K.A., Vine, F.J., 2009. Global Tectonics. John Wiley & Sons.
Korenaga, J., 2020. Plate tectonics and surface environment: Role of the oceanic upper mantle. Earth-Sci. Rev. 205, 103185.
Kuang, W., Yuan, C., Zhang, J., 2021. Real-time determination of earthquake focal mechanism via deep learning. Nat. Commun. 12, 1432. doi:10.1038/s41467-021-21670-x.
Kusky, T.M., 2008. Earthquakes: Plate Tectonics and Earthquake Hazards. Infobase Publishing.
Le Grand, H.E., 1988. Drifting Continents and Shifting Theories. Cambridge University Press.
Le Pichon, X., 1968. Sea-floor spreading and continental drift. J. Geophys. Res. 73, 3661–3697.
Lee, W.H.K., Wu, F.T., Jacobsen, C., 1976. A catalog of historical earthquakes in China compiled from recent Chinese publications. Bull. Seismol. Soc. Am. 66, 2003–2016.
Lin, C.-W., Shieh, C.-L., Yuan, B.-D., Shieh, Y.-C., Liu, S.-H., Lee, S.-Y., 2004. Impact of Chi-Chi earthquake on the occurrence of landslides and debris flows: example from the Chenyulan River watershed, Nantou, Taiwan. Eng. Geol., Reconnaiss. Chi-Chi Earthq., Taiwan 71, 49–61. doi:10.1016/S0013-7952(03)00125-X.
List of historical earthquakes, 2021. Wikipedia.
Lomnitz, C., 2013. Global Tectonics and Earthquake Risk. Elsevier.
Manepalli, U.R., Bham, G.H., Kandada, S., 2011. Evaluation of hotspots identification using kernel density estimation (K) and Getis-Ord (Gi*) on I-630. In: 3rd International Conference on Road Safety and Simulation, pp. 14–16.
Masum, M., Akbar, M.A., 2019. The pacific ring of fire is working as a home country of geothermal resources in the world. IOP Conference Series: Earth and Environmental Science, 249 doi:10.1088/1755-1315/249/1/012020.
McCloskey, J., Antonioli, A., Piatanesi, A., Sieh, K., Steacy, S., Nalbant, S., Cocco, M., Giunchi, C., Huang, J., Dunlop, P., 2008. Tsunami threat in the Indian Ocean from a future megathrust earthquake west of Sumatra. Earth Planet. Sci. Lett. 265, 61–81.
Miyazaki, S., Segall, P., Fukuda, J., Kato, T., 2004. Space time distribution of afterslip following the 2003 Tokachi-oki earthquake: implications for variations in fault zone frictional properties. Geophys. Res. Lett. 31.
Molnar, P., 1979. Earthquake recurrence intervals and plate tectonics. Bull. Seismol. Soc. Am. 69, 115–133.
Monecke, K., Finger, W., Klarer, D., Kongko, W., McAdoo, B.G., Moore, A.L., Sudrajat, S.U., 2008. A 1,000-year sediment record of tsunami recurrence in northern Sumatra. Nature 455, 1232–1234.
Morgan, W.J., 1968. Rises, trenches, great faults, and crustal blocks. J. Geophys. Res. (1896-1977) 73, 1959–1982. doi:10.1029/JB073i006p01959.
Mulargia, F., Bizzarri, A., 2014. Anthropogenic triggering of large earthquakes. Sci. Rep. 4, 1–7.
Nanjo, K.Z., 2020. Were changes in stress state responsible for the 2019 Ridgecrest, California, earthquakes? Nat. Commun. 11, 3082. doi:10.1038/s41467-020-16867-5.
Nur, A., Cline, E.H., 2000. Poseidon's horses: plate tectonics and earthquake storms in the Late Bronze Age Aegean and Eastern Mediterranean. J. Archaeol. Sci. 27, 43–63.
Okal, E.A., Synolakis, C.E., 2008. Far-field tsunami hazard from mega-thrust earthquakes in the Indian Ocean. Geophys. J. Int. 172, 995–1015. doi:10.1111/j.1365-246X.2007.03674.x.
Olsen, P.E., 1997. Stratigraphic record of the early Mesozoic breakup of Pangea in the Laurasia-Gondwana rift system. Annu. Rev. Earth Planet. Sci. 25, 337–401.
Olson, H.J., 1989. Small Scale Geothermal Development Potential for Island Nations Situated Along the Pacific" Ring of Fire".
Pal, I., Nath, S.K., Shukla, K., Pal, D.K., Raj, A., Thingbaijam, K.K.S., Bansal, B.K., 2008. Earthquake hazard zonation of Sikkim Himalaya using a GIS platform. Nat. Hazards 45, 333–377. doi:10.1007/s11069-007-9173-7.
Pal, I., Tularug, P., Jana, S.K., Pal, D.K., 2018. Chapter 17 - risk assessment and reduction measures in landslide and flash flood-prone areas: a case of southern Thailand (Nakhon Si Thammarat Province). In: Samui, P., Kim, D., Ghosh, C. (Eds.), Integrating Disaster Science and Management. Elsevier, pp. 295–308. doi:10.1016/B978-0-12-812056-9.00017-8.
Palin, R.M., Santosh, M., 2020. Plate Tectonics: What, Where, Why, and When?. Gondwana Research.
Papadopoulos, G.A., Vassilopoulou, A., 2001. Historical and Archaeological Evidence of Earthquakes and Tsunamis Felt in the Kythira Strait, Greece, in: Tsunami Research at the End of a Critical Decade. Springer, pp. 119–138.
Parsons, A.J., Hosseini, K., Palin, R., Sigloch, K., 2020. Geological, geophysical and plate kinematic constraints for models of the India-Asia collision and the post–Triassic central Tethys oceans. Earth-Sci. Rev. 208 (103084).
Parwanto, N.B., Oyama, T., 2014. A statistical analysis and comparison of historical earthquake and tsunami disasters in Japan and Indonesia. Int. J. Dis. Risk Reduct. 7, 122–141.
Paton, D., Jang, L., 2016. Earthquake readiness and recovery: an Asia-Pacific perspective. In: Earthquakes and Their Impact on Society. Springer, pp. 647–663.
Piper, J.D.A., Briden, J.C., Lomax, K., 1973. Precambrian Africa and South America as a single continent. Nature 245, 244–248.
Pollitz, F.F., Stein, R.S., Sevilgen, V., Bürgmann, R., 2012. The 11 April 2012 east Indian Ocean earthquake triggered large aftershocks worldwide. Nature 490, 250–253. doi:10.1038/nature11504.

Prasannakumar, V., Vijith, H., Charutha, R., Geetha, N., 2011. Spatio-temporal clustering of road accidents: GIS based analysis and assessment. Proc.-Soc. Behav. Sci. 21, 317–325.
Pritchard, M.E., Jay, J.A., Aron, F., Henderson, S.T., Lara, L.E., 2013. Subsidence at southern Andes volcanoes induced by the 2010 Maule, Chile earthquake. Nat. Geosci. 6, 632–636.
Rathore, N.S., 2003. Evolution of the earth and occurrence of earthquakes. In: Proceedings of the KSRS Conference, pp. 369–371.
Rychert, C.A., Harmon, N., 2021. Fluid-rich extinct volcanoes cause small earthquakes beneath New Zealand.
Satake, K., Shimazaki, K., Tsuji, Y., Ueda, K., 1996. Time and size of a giant earthquake in Cascadia inferred from Japanese tsunami records of January 1700. Nature 379, 246–249.
Schorlemmer, D., Wiemer, S., Wyss, M., 2005. Variations in earthquake-size distribution across different stress regimes. Nature 437, 539–542. doi:10.1038/nature04094.
Sekac, T., Jana, S., Pal, I., Pal, D., 2016a. GIS based evaluation in earthquake hazard micro-zonation -a case study of madang and morobe province, Papua New Guinea. Int. j. adv. eng. res. sci. 3, 95–104.
Sekac, T., Jana, S., Pal, I., Pal, D., 2016b. A GIS based approach into delineating liquefaction susceptible zones through assessment of site-soil-geology-A case study of Madang and Morobe province in Papua New Guinea (PNG). Int. J. Innovat. Res. Sci., Eng. Technol. 5, 6616–6629. doi:10.15680/IJIRSET.2016.0501003.
Sekac, T., Jana, S.K., Pal, I., Pal, D.K., 2020. Application of geospatial technology in earthquake risk assessment in Papua New Guinea. In: Pal, I., von Meding, J., Shrestha, S., Ahmed, I., Gajendran, T. (Eds.), An Interdisciplinary Approach for Disaster Resilience and Sustainability, Disaster Risk Reduction. Springer, Singapore, pp. 185–218. doi:10.1007/978-981-32-9527-8_12.
Sekac, T., Jana, S.K., Pal, I., Pal, D.K., 2016c. Earthquake hazard assessment in the Momase region of Papua New Guinea. Spat. Inf. Res. 24, 617–637. doi:10.1007/s41324-016-0058-2.
Silva, R., França, G.S., Vilar, C.S., Alcaniz, J.S., 2006. Nonextensive models for earthquakes. Phys. Rev. E 73, 026102. doi:10.1103/PhysRevE.73.026102.
Singh, A.P., Mishra, O.P., 2015. Seismological evidence for monsoon induced micro to moderate earthquake sequence beneath the 2011 Talala, Saurashtra earthquake, Gujarat, India. Tectonophysics 661, 38–48. doi:10.1016/j.tecto.2015.07.032.
Smith, D.K., Escartin, J., Cannat, M., Tolstoy, M., Fox, C.G., Bohnenstiehl, D.R., Bazin, S., 2003. Spatial and temporal distribution of seismicity along the northern Mid-Atlantic Ridge (15°–35°N). J. Geophys. Res.: Solid Earth 108. doi:10.1029/2002JB001964.
Socquet, A., Simons, W., Vigny, C., McCaffrey, R., Subarya, C., Sarsito, D., Ambrosius, B., Spakman, W., 2006. Microblock rotations and fault coupling in SE Asia triple junction (Sulawesi, Indonesia) from GPS and earthquake slip vector data. J. Geophys. Res.: Solid Earth 111.
Strahler, A.N., Strahler, A.H., 1976. Elements of Physical Geography. Wiley.
Suárez, G., García-Acosta, V., Gaulon, R., 1994. Active crustal deformation in the Jalisco block, Mexico: evidence for a great historical earthquake in the 16th century. Tectonophysics 234, 117–127.
Swift, S.A., Carr, M.J., 1974. The segmented nature of the Chilean seismic zone. Phys. Earth Planet. Inter. 9, 183–191.
Varo, J., Sekac, T., Jana, S., 2019a. Landslide hazard zonation from a GIS perspective and urban planning solutions in central –division of Fiji Islands. Int. J. Innovat. Technol. Expl. Eng. 8. doi:10.35940/ijitee.L1091.10812S19.
Varo, J., Sekac, T., Jana, S.K., 2019b. Earthquake hazard micro zonation in Fiji Islands: a research of VitiLevu Island.
Varo, J., Sekac, T., Jana, S.K., Pal, D.K., 2019b. Demarcation of liquefaction zones and risk reduction in Fiji Islands from a geomatics perspective: a case study of Viti Levu Island. Spat. Inf. Res. 27, 643–658.
Vishnu, S., Srinu, U., 2014. Potential of fractal analysis of earthquakes through wavelet analysis and determination of b value as an aftershock precursor: a case study using earthquake data between 2003 and 2011 in Turkey. J. Earthq. 2014. doi:10.1155/2014/123092.
Wan, B., Yang, X., Tian, X., Yuan, H., Kirscher, U., Mitchell, R.N., 2020. Seismological evidence for the earliest global subduction network at 2 Ga ago. Sci. Adv. 6, eabc5491.
Watt, S.F., Pyle, D.M., Mather, T.A., 2009. The influence of great earthquakes on volcanic eruption rate along the Chilean subduction zone. Earth Planet. Sci. Lett. 277, 399–407.
Wegener, A., 1912. Die entstehung der kontinente. Geol. Rundsch. 3, 276–292.
Weischet, W., Huene, R.V., 1963. Further observations of geologic and geomorphic changes resulting from the catastrophic earthquake of May 1960, in Chile. Bull. Seismol. Soc. Am. 53, 1237–1257. doi:10.1785/BSSA0530061237.
Wilson, J.T., 1968. Static or mobile earth: the current scientific revolution. Proc. Am. Philos. Soc. 112, 309–320.
Wilson, J.T., 1965. A new class of faults and their bearing on continental drift. Nature 207, 343–347.
Wilson, M.P., Foulger, G.R., Gluyas, J.G., Davies, R.J., Julian, B.R., 2017. HiQuake: the human-induced earthquake database. Seismol. Res. Lett. 88, 1560–1565.
Woodcock, N.H., 1986. The role of strike-slip fault systems at plate boundaries. Philos. Trans. R. Soc. Lond. Ser. A, Math. Phys. Sci. 317, 13–29.